WIND TUNNEL SIMULATION OF ATMOSPHERIC BOUNDARY LAYER FLOWS

Pedro H. de A. Barbosa, Marcio Cataldi, and Atila P. Silva Freire
Mechanical Engineering Program (PEM/COPPE/UFRJ),
C.P. 68503, 21945-970 - Rio de Janeiro - Brazil.

Abstract. *The present work discusses various types of turbulence generators which can be used to generate thick turbulent boundary layers. The experimental assessment of the generators was carried out considering the integral properties of the flow, skin-friction, mean velocity profiles in inner and outer coordinates and turbulence. Designs based on triangular wedge, elliptic wedge and cylindrical rod generators are analyzed. The paper describes in detail the experimental arrangement, including the features of the wind tunnel and of the instrumentation. The results are compared with naturally developed flow and with experimental data from other authors.*

Key words: *Turbulence, roughness, boundary layer, atmospheric flows*

1. INTRODUCTION

The fluid mechanics of winds has been studied in the past by two basic approaches: physical modelling and numerical modelling. The physical modelling in wind tunnels presents, in particular, a great flexibility for the simulation of atmospheric boundary layers (ABL) subjected to realistic surface conditions. Unfortunately, the simulation of ABL effects in an controlled environment is normally an expensive task since it may require the use of wind tunnels with very long test-section. A useful way to extend the range of operation of short wind tunnels consists in obtaining, through artificially thickened boundary layers, velocity profiles that resemble ABL profiles after some downstream distance from the thickening device.

Thick boundary layers can be created through several artificies; for instance, the paper of Hunt and Fernholz(1975) lists ten possible methods of simulation of neutral, stable and unstable atmospheric conditions in various types of wind tunnel. These methods vary greatly in sophistication and in working principia so that their full undestanding and applicability has not as yet been unveiled.

An apparently simple way of generating a thick boundary layer is to force the flow to pass through a combination of spires, wedges or trips together with roughness elements

distributed on the wall. From the 28 wind tunnels scrutinized by Hunt and Fernholz(1975), 11 resort to vorticity generators, 23 to roughness elements and 15 to fences. In fact, 9 facilities resort to a combination of all these three simulation methods; this only emphasizes their importance.

Unfortunately, since these popular simulation methods are complicated enough from a fluid mechanics point of view, they have encouraged researchers to choose an adequate geometry by trial and error. The works of Counihan(1969) and of Ligrani et al.(1979, 1983), for example, describe thickening devices which are neetly built with a very sophisticated geometry that requires fine mechanics to be manufactured. Their construction, therefore, is time consuming and frequently costly. This fact is much aggravated by the uncertainty related to their applicability in a different wind tunnel environment from that to which they were originarilly designed.

In a previous work, Guimaraes et al.(1999) have shown how a combination of spires and trips can be used to produce thick boundary layers with characteristics similar to the atmospheric boundary layer. Five different geometrical arrangements were presented to produce boundary layers of thickness varying from 9 to 18 cm. The geometries were much simpler than those presented by Counihan(1969) and by Ligrani et al.(1979, 1983) resulting from simple compositions prepared from rods and bars. Thus, at that time, the main objective of the work was to develop simple means to artificially increase the boundary layer thickness. The boundary layer was qualified by examining the following features: growth, structure, equilibrium and turbulent transport of momentum. These properties were compared with the properties that would result from a naturally developed boundary layer of the same thickness.

The purpose of this work is to extend the results of Guimaraes et al.(1999) to a further range of validity. In other words, the work aims at producing artificial boundary layers with thickness up to 27 cm. More than that, the work aims at producing boundary layers with a higher quality than those presented in Guimaraes et al.(1999); boundary layers that present properties closer to a naturally developed boundary layer in relation to the qualification parameters described above and also in relation to the longitudinal spectrum.

In what follows, a short review on the techniques used to thicken the boundary layer will be presented. Next, the experimental apparatus and procedure will be described. The experimental results and comparison with other works are given in section four.

2. SIMULATION METHODS

As mentioned in Guimaraes et al. (1999) several techniques have been used to artificially thicken boundary layers. Typical examples are the use of fences, uniform grids, graded or sheared grids, jets, pulsation, wall roughness, steps, screens, vortex generators and thermal stratification (Hunt and Fernholz (1975)).

Normally, these techniques are divided into three categories:

1. Alteration of the surface conditions by the use of roughness or boundary layer trips.

2. Alteration of both the inner and the outer regions of the boundary layer by directional jets placed in the floor at the entrance of the working section or by multiple horizontal jets of variable strength directed at each other from either side of the wind tunnel.

3. Alteration of the external irrotational flow by spires extending all the way from the wall to the oncoming flow. The turbulent wakes formed by the spires convect downstream to merge with the existing boundary layer resulting in a new structure which, in some cases, may resemble a thick boundary layer.

Kline et al.(1967) have shown that, in a turbulent boundary layer, production plays a primary role in defining the turbulence structure. In a normally developed boundary layer, the overall structure results from large scale structures originated from the interaction between eddies formed by near-wall turbulent bursts and by the inflow of high-speed flow towards the wall. The bursts are very likely provoked by a strong instability mechanism and play a fundamental role in transporting turbulent kinetic energy to the outer region of the boundary layer.

Thus, according to this picture, the structure of the flow downstream of the spires will result from the mixing between the organized large eddy motion generated by the wakes of the spires and the violent ejection of low-speed fluid from the very near wall regions. Hence, before the flow is likely to conform to the boundary layer properties, a sufficient degree of mixing must be assured to it so that the lifetime of the large eddy wake structures is exceeded.

All the above puts a lot of emphasis on the idea that the wall layer streak formation and break up play the central role in determining the structure of the turbulent boundary layer and that for this reason the details of the wake flow behind the spires exert a minor role on the process.

The spires designed in the mid sixties were based on different principia; they intended to produce a model flow based on the existence of sets of large eddies in both the inner and the outer regions of the boundary layer. Triangular generators with pairs of surfaces at alternate incidences were designed to produce large vortices of opposite sign of the type envisaged by Townsend(1957). These vortices should accelerate the outward diffusion of the high intensity turbulence produced at ground level.

Experiments using triangular generators indicated a tendency for an excessive momentum loss in the inner region of the boundary layer and an insufficient loss in the outer region. In an attempt to resolve this, elliptic generators were tried. Elliptic generators were designed to keep turbulence constant with height or, more acceptable, to produce turbulence levels that decayed from some maximum value near the wall to approximately zero at the edge of the shear flow. The side view of the elliptic wedge generators presented by Counihan(1969) is of a quarter ellipsis whose major axis is twice the length of the minor axis. The plan view of the generator is wedge shaped; the apex of the wedges faces the flow. Two types of wedges with constant angles of 5^o and 6^o were tested. The final assessment was based on measurements of the distribution of longitudinal turbulence in the wake of single generators. A spanwise variation of turbulence of the order of 1% was required at any given height in the boundary layer.

Ligrani et al.(1979, 1983) used streamlined spires with sharp-edged upstream and downstream blades. The total angle of the upstream blade was carefully adjusted for a fine tuning of the fluctuation intensities. A cross barrier set downstream of the spires was used to increses the momentum deficit over that resulted from the spires alone.

3. EXPERIMENTAL APPARATUS

In the present work, it was decided that simple geometrical elements would be summouned for the construction of the thickening device. Following the procedure of Guimaraes et al.(1999) two basic components were used: cylindrical rods and rectangular bars. Different combinations of these two elements were studied to produce many different types of geometries. In all configurations, an array of rods which extended across the width of the wind tunnel was used. A rectangular bar located on the downstream side of the rods was also used to achieve normal turbulence structure. As the flow approached the rods, a trip was placed over the wall.

The main advantage of the present geometry was really its simplicity. However, because the rods had a constant diameter, controlling the level of turbulence was very difficult. The general features of the present design were taken from Ligrani et al.(1983), who in turn based their design on an apparatus developed by Cermak(1971), Peterka and Cermak(1974) and Cermak(1975) to simulate the atmospheric boundary layer.

The shape and location of the components were determined through trial and error. In fact, before we arrived at the present geometry, several attempts were made. In our first try, screens were used; they resulted, however, in very distorted velocity profiles. Basically, the aerodynamic drag of the screens was too high so that a strong blockage effect was achieved resulting in a strong acceleration of the flow in the top part of the tunnel. Elliptic wedge generators were also tried. For that matter, we followed the design proposed by Couhinan(1969). Contrary to this author, we took our measurements 2300 mm downstream of the generators instead of 450 mm. To our disappointment, a flow with an exaggerated wake region was found. Then, based on the previous experience of Guimaraes et al.(1999), we decided to go back the to combination of rods and bars.

The two final geometrical configurations of the thickening apparatus are shown in Figures 1 and 2.

Figure 1: Thickening device for 80 mm rods.

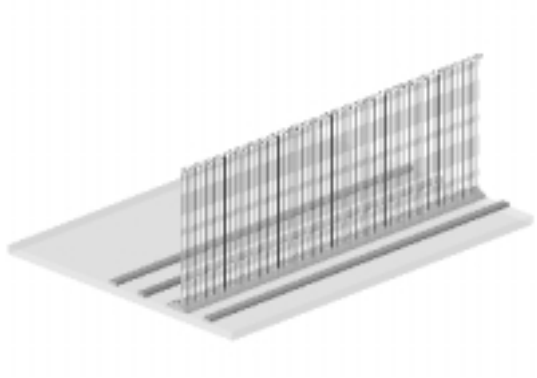

Figure 2: Thickening device for 160 mm rods.

In Figures 1 and 2, the thickening devices are shown in position. The rods were made by cutting cylindrical 1/8" thick bars in two different heights: 80 mm and 160 mm. In the final configuration for the 80 mm rods, an optimal arrangement was found by placing each rod 10 mm apart from each other. In our case, 66 rods were used to achieve the expected effect. A rectangular (15 mm x 5 mm) aluminium bar (trip), transversal to the mean flow, also was used. For both configurations, the trip was placed 50 mm far upstream

from the rods as shown in Figures 1 and 2. For the 160 mm rods, an optimal arrangement only was reached when each rod was spaced 7 mm from each other. To achieve this, 95 rods were used. Two identical trips were positioned, respectively, at 80 mm and 150 mm downstream from the rods; also a 1/8" cylindrical bar was placed at the top of the rods as shown in Figure 2.

The thickening apparatuses were tested for just one freestream velocity. The wind tunnel used was the high turbulence wind tunnel located at the Laboratory of Turbulence Mechanics of the Mechanical Engineering Program of COPPE/UFRJ; for flows over a uniformly smooth surface, the free stream level of turbulence was about 2%. The tunnel is an open circuit tunnel with a test section of dimensions 670x670x3000 mm; the test section has a roof with adjustable inclination to assure the flows to have a zero pressure gradient.

Measurements were performed for values of the free-stream velocity of 3.00 m/s. Mean velocity profiles and turbulence intensity levels were obtained using a constant temperature hot-wire anemometer. The boundary layer probe was of the type 55P11. A Pitot tube, an electronic manometer, and a computer controlled traverse gear were also used. In getting the data, 27,000 samples were considered which yielded an accuracy of 3% in the mean velocity data.

To obtain accurate measurements, the mean and fluctuating components of the analogic signal given by the anemometer were treated separately. Two output channels of the anemometer were used. The mean velocity profiles were calculated directly from the untreated signal of channel one. The signal given by channel two was 1 Hz high-pass filtered leaving, therefore, only the fluctuating velocity. The latter signal was then amplified with a gain controlled between 1 and 500 and shifted by an offset so as to adjust the amplitude of the signal to the range of the A/D converter.

4. EXPERIMENTAL ASSESSMENT OF THE GENERATORS

The assessment was carried out considering the integral properties of the flow, skin-friction, mean velocity profiles in inner and outer coordinates and turbulence.

4.1. Integral properties

The boundary layer growth can be characterized through variation of the momentum thickness with the downstream distance, and through variation of the skin-friction coefficient with the momentum thickness.

The momentum thickness was evaluated directly from the mean velocity profile through a simple numerical quadrature. The results are shown in Figure 3. The effective velocity boundary layer starting distance upstream of the rods was determined based on the momentum thickness correlation

$$\delta_2 = 0.036\, x \left(\frac{U_\infty x}{\nu}\right)^{-1/5}. \qquad (1)$$

The calculated skin-friction results are shown in Figure 4. The values of C_f were determined directly from the velocity profiles through the gradient of the logarithmic profile. The data results show a good agreement when compared with $C_f/2 = 0.0128\, R_{\delta_2}^{-0.25}$.

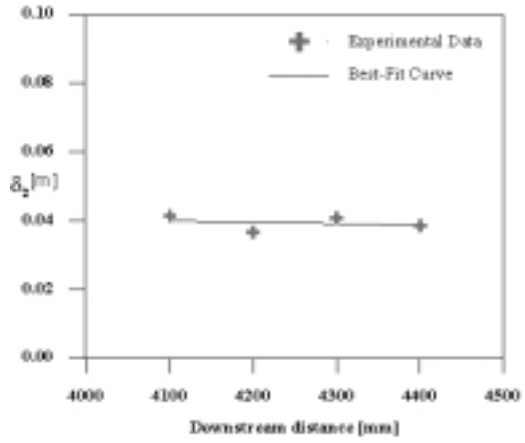

Figure 3: Momentum thickness for 160 mm rods.

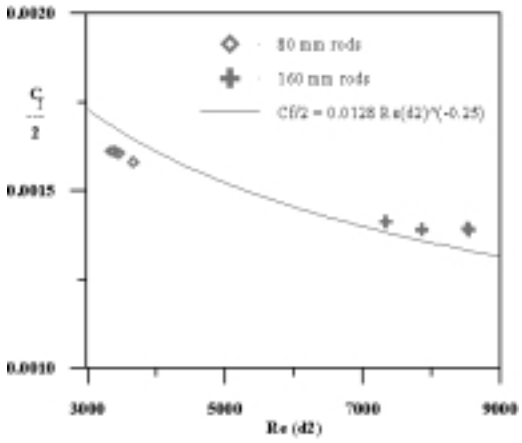

Figure 4: Skin-friction results.

The extent in origin is shown in Table 1. The extent in origin represents the distance that a naturally developed boundary layer would need to flow so that its properties would achieve the values measured here.

Table 1: Upstream extent in origin.

Configuration	Station (mm)	Origin Location
1	2100	8.75 m
1	2200	8.66 m
1	2300	8.64 m
1	2400	8.57 m
2	4100	25.49 m
2	4200	21.60 m
2	4300	25.09 m
2	4400	23.18 m

4.2. Local properties

Velocity profiles plotted in wall coordinates are shown in Figures 5 and 6. This Figure was prepared with values of C_f obtained through the graphical method of Clauser, that is, through the inclination of the velocity profiles in the fully turbulent region of the flow.

In all cases they were compared with the classical law of the wall formulation

$$\frac{u}{u_\tau} = \frac{1}{\varkappa} \ln \frac{y u_\tau}{\nu} + A, \tag{2}$$

where $\varkappa = 0.4$ and $A = 5.0$. The resulting values of A are shown in Table 2.

For large values of $y u_\tau / \nu$, the velocity profile starts to depart from the law of the wall giving form to the law of the wake. In wake coordinates, the velocity profiles show good agreement with the law of the wake of Coles (Figures 7 and 8). The velocity profiles were also approximated by a power-law profile. The resulting value for the exponent, n, is

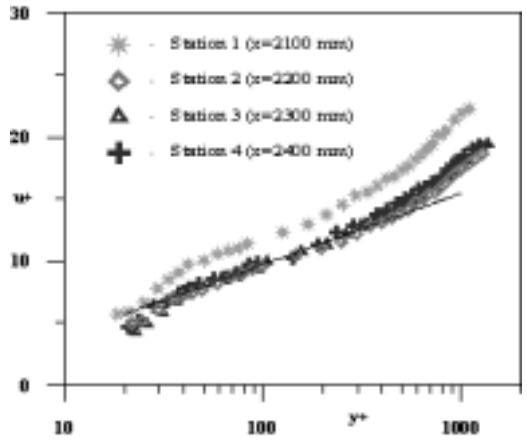

Figure 5: Velocity profiles in inner coordinates for 80 mm rods.

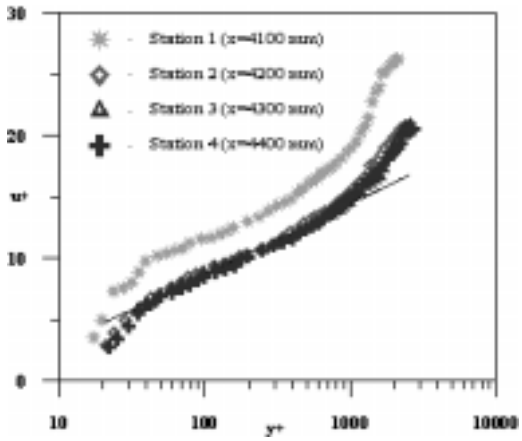

Figure 6: Velocity profiles in inner coordinates for 160 mm rods.

Table 2: Linear coefficient in law of the wall.

Configuration	Station (mm)	A
1	2100	5.64
1	2200	4.08
1	2300	5.87
1	2400	4.34
2	4100	4.00
2	4200	6.11
2	4300	4.54
2	4400	3.75

shown in Table 3 compared with wind data collected from 19 different sites as presented by Davenport(1960, 1963). This exponent was obtained through a best-fit interpolation of the mean velocity profiles for the 160 mm rods. As can be observed in Table 3, our velocity profiles resemble more an urban ABL than a rural ABL.

The Clauser shape factor G, defined as

$$G = \frac{\int_0^\infty \frac{U_\infty - U}{u_\tau}\, dy}{\int_0^\infty \left(\frac{U_\infty - U}{u_\tau}\right)^2 dy}, \tag{3}$$

is shown in Figures 9 and 10. For most of the configurations, the experimental G was found to lie about a near constant value, indicating an equilibrium condition for the boundary layer.

When the first velocity profiles were obtained for the 16 mm rods, the defect region of the boundary layer presented a deficit in velocity which was thought by the present authors to be excessive. To correct this effect, the test section of the wind tunnel was extended from 3000 mm to 5000 mm. After experimental verification, it was in fact confirmed that the additional 2 meters were sufficient for a further mixing of the flow to conform the boundary layer to the desired properties.

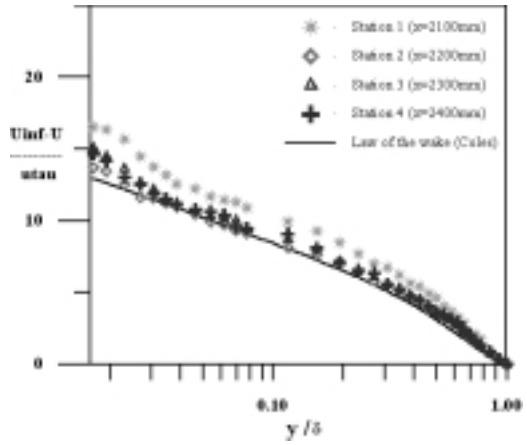

Figure 7: Velocity profiles in outer coordinates for 80 mm rods.

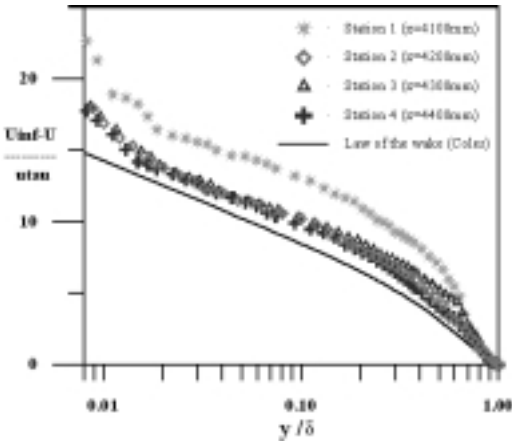

Figure 8: Velocity profiles in outer coordinates for 160 mm rods.

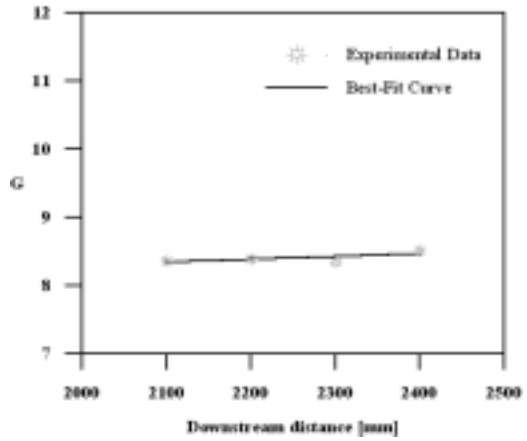

Figure 9: Clauser factor for 80 mm rods.

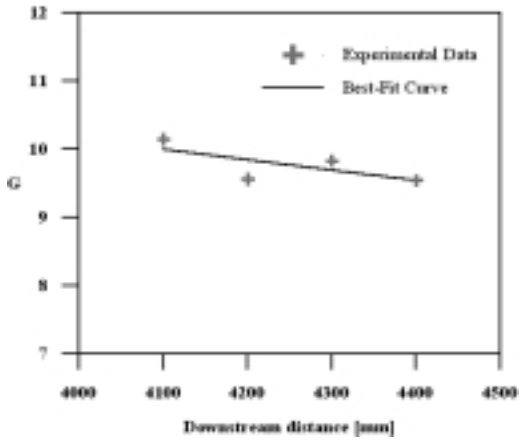

Figure 10: Clauser factor for 160 mm rods.

5. Longitudinal turbulence

Qualification of the artificially thickened boundary layer will include the longitudinal turbulence spectrum. Measurements made for 80 mm rods are shown in Figure 11.

The spectral magnitudes are normalized according to

$$\int_0^\infty \frac{F_u(k)}{y}\, d(yk) = 1.0 \tag{4}$$

where k denotes the one-dimensional wavenumber. As can be seen in Figure 11, the longitudinal turbulence spectrum for all stations seems to be in a good agreement with the Kolmogorov's empirical $k^{-5/3}$ decay law. It can also be noted that, as the downstream distance from the thickening device increases, the energy peak decreases; this fact was first observed by other authors in a turbulent homogeneous flow.

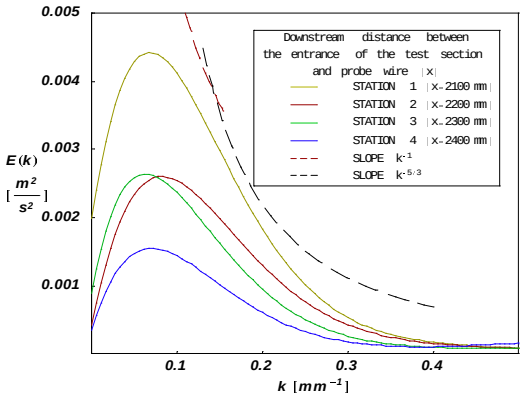

Figure 11: Longitudinal turbulence spectra for 80 mm rods.

6. Data analysis

This section, which was first shown in Guimaraes et al.(1999), is here presented again. It contains a comparison between our results and data obtained in other wind tunnels. In addition, some ABL features at three different conditions are also included.

Table 3: Wind tunnel simulation systems and ABL features.

Institution	W-T dim.(m)	S.M.	MS/FS	$\delta(m)$	n	u_τ/U_∞	IT%
Vienna	1.7x1.2x10	F, R	1/200	0.6	–	–	–
Bochum	2.1x2.1x4.3	F, V, R	1/500	0.84	–	–	–
Marseille	3.2x1.5x40	R, T	1/20	0.75	–	0.045	2.0
Poitiers	5.5x5.3x26	GG, R, T	1/200	2.5	–	–	–
Edinburgh	1.5x0.9x9	V,Sc,R	1/350	0.7	0.36	0.05	1.8
Salford	0.5x0.5x1	UG,GG,Sc	–	0.4	–	–	–
Stevenage	4.3x1.5x22	F, V, R	1/50	1.0	–	0.055	1.8
Notre Dame	1.5x1.5x14	J, R T	1/100	1.0	–	0.044	3.1
COPPE/UFRJ	0.67x0.67x5	V, R	–	0.27	0.31	0.048	2.0
Rural A.B.L	–	–	–	500	0.16	0.03	2.6
Urban A.B.L.	–	–	–	600	0.4	0.05	2.6
Over Sea A.B.L.	–	–	–	280	0.15	–	8.0

Key to table: W-T, wind tunnel; S.M., simulation method; MS/FS, model scale over full scale; n, exponent of the power-law profiles; A.B.L, atmospheric boundary layer; F, fences; GG, graded or shear grids; UG, uniform grids; J, jets; R, roughness; Sc, screens; T, thermal stratification; V, vortex or vorticity generators.

7. Conclusion

As corroborated by the data presented in the previous sections, the results obtained at the high-turbulence wind-tunnel located at COPPE/UFRJ stand reasonably well against a comparison with wind tunel data published by other authors and with the empirical theories collected from literature. The main contribution of the work has been to identify a simple geometrical arrangement which is capable of generating very thick turbulent

boundary layers with properties very close to normal properties. Although it was not a primarly intend of the authors, this work has also identified for these arrangements a minimum required length for neutral ABL simulation at the COPPE/UFRJ wind tunnel. In both configurations, at Station 1, the flow did not achieve a sufficient degree of mixing to produce a thick boundary layer profile with normal properties. This behavior was confirmed when mean velocity profiles were plotted in both inner and outer coordinates for rods with 80 and 160 mm (Figures 5 to 8).

The job of reproducing exactly in a laboratory the features of the atmospheric boundary layer is a very difficult problem which demands time and resources. In a previous work, Guimaraes et al.(1999) have achieved qualified boundary layers with thicknesses up to 13 cm. Here we have further extended this range to 27 cm. When this work started the objective was to produce qualified boundary layers with a thickness of 40 cm. Unfortunately, with the previous 3000 mm long working section, only thicknesses up to 16 cm could be obtained. The goal of obtaining thicker boundary layers then prompted us to increase the length of the working section to 5000 mm.

At the present stage, the research continues since our objective of obtaining 40 cm thick boundary layers remains. Any progress will be reported later.

Acknowledgements. The present work was financially supported by the Brazilian National research Council – CNPq – through grant No 350183/93-7.

REFERENCES

Cermak, J. E.; 1971, A.I.A.I. J., vol. 9, pp. 1746.

Cermak, J. E.; 1975, J. Fluids Engineering, vol. 97, pp. 9.

Counihan, J.; 1969, J. Fluid Mechanics, vol. 3, pp. 197–214.

Davenport, A. G.; 1960, N.P.L., U.K., pp. 54–83.

Davenport, A. G.; 1963, Proceedings ASCE, Journal of the Structural Division, vol. 86, pp. 39–66.

Guimaraes, J. H. D., dos Santos, S. J. F., Jr., Su, J. and Silva Freire, A. P.; 1999, Proceedings of the 15th Brazilian Congress of Mechanical Engineering (COBEM99).

Hunt, J. C. R. and Fernholz, H.; 1975, J. Fluid Mechanics, vol. 70, pp. 543–559.

Kline, S. J., Reynolds, W. C., Schraub, F. A. and Runstadler, P. W.; 1967, J. Fluid Mechanics, vol. 30, pp. 741–773.

Ligrani, P. M., Moffat, R. J. and Kays, W. M., 1979, Report No HMT-29, Stanford University.

Ligrani, P. M., Moffat, R. J. and Kays, W. M., 1983, J. Fluids Engineering, vol. 105, pp. 146-153.

Peterka, J. A. and Cermak, J. E; 1974, CER 73-74JAP-JEC2, Fluid Mechanics Program, Colorado State University.

Townsend, A. A.; 1957, Proc. I.U.T.A.M. Symposium on Boundary Layer Research, Springer, Berlin.